*International Journal of Engineering &Technology*, 13 (1) (2024) 156-166

International Journal of Engineering & Technology

*Website: www.sciencepubco.com/index.php/IJET*

***Research paper***

# Mathematical models of power transformers winding faults diagnosis based on voltage-current characteristics

**Ftatsi Mbetmi Guy-de-patience [1, 2], Tsegaing Tchatchueng Fabrice [1, 2], Boussaibo Andre [1, 2], Sametah Macine Ngong [2], Ndjiya Ngasop Stephane [2] ***

[1] *Laboratory of Analyses, Simulations and Testing (LASE), University Institute of Technology, University of Ngaoundere, Cameroon*
[2] *Laboratory of Energy, Signal, Images and Automatic (LESIA), National School of Agro-Industrial Sciences (ENSAI), University of Ngaoundere, Cameroon*
**Corresponding author E-mail: ndjiyangasop@yahoo.fr*

**Abstract**

Power transformers are important components of electrical systems. Their failures are very costly, mainly because of the unavailability of electrical service they cause. Rapid and accurate diagnosis of internal transformer faults is a key factor of efficient and safe operation. Such diagnosis is usually carried out by experts. Several methods of power transformer windings diagnosis exist. The online diagnosis, the interpretation of results and the identification of various internal winding faults are criteria to be taken into account when choosing a method. The voltage-current method is a powerful method that has been successfully used as a diagnostic technique to detect power transformer winding faults. In this work we propose a mathematical models of power transformers winding faults based on voltage-current method. To achieve our goal, we modelled the transformer winding as a distributed network of similar R-L-C circuits. Then we used Matlab/Simulink to simulate the different winding faults on a number of discs ranging from 5 to 120. We defined four failures indicators and we studied their evolution for each fault. At the end we give for each fault the corresponding mathematical model. The transformer used in this work is a 15 MVA 22/0.415 kV distribution power transformer.

***Keywords***: *Distribution Power Transformer; Diagnosis; Voltage–Current; Indicators Semicolon.*

## 1. Introduction

The reliability and the safety operation of electrical networks are major issues for energy suppliers' company, since most unplanned shutdowns can cause very serious economic consequences. In electrical networks, the voltages are fixed by power transformers. These transformers are capable of supporting power ratings up to several hundred MVA. Given the current economic challenges, energy supply companies invest considerable resources in maintenance operations. These maintenance operations aim to increase reliability, extend the life of transformers, minimize failures and limit unavailability. A study of 536 failed power transformers shows that the main cause of transformers failure is due to their windings [1]. Based on this observation, several research projects have been carried out with the aim of providing maintenance solutions for power transformer windings. We can name: Frequency Response Analysis (FRA) [2-5], Analysis of sequences negative current [6], Voltage–Current locus diagram (V-I) [7-9], Temperature measurement [10], [1] and flux-based method [11-12]. Table 1 present a brief comparison between V-I method and other mentioned methods. The FRA technique requires expert personnel to determine the type and possible location of the fault [13]. Analysis of sequences negative current, temperature measurement and flux-based method have easy to interpret results but can't identify various internal winding faults. The voltage-current technique as presented in [14], [9] relies on constructing a locus diagram relating the transformer input current of a particular phase on the x-axis and the difference between the input and output voltages of the same particular phase on the y-axis. This allows the modelling of only one winding of the transformer. In this paper we extend the method to two windings. The current in one primary winding of the transformer is considered as the x-axis, and the voltage difference between the same primary winding and particular secondary winding is considered as the y-axis. This allows us modelling two winding of the power transformer (the primary and the secondary). Then we define four failures indicators and we both study their evolution for each fault and give the corresponding mathematical model.

## 2. Transformer model

The transformer has been modelled as a distributed network of similar R-L-C circuits (Fig. 1.). This model is used in the FRA but can also be used in voltage-current diagram method as presented in [7] and [9]. A winding consists of a number of elements called discs. Every disc consists of a number of turn and has an internal resistance, capacitance and inductance. In the model of figure 1 r and r' are respectively the series resistances per disc of the High Voltage and Low Voltage winding; Cg and Cg' are respectively the ground capacitance per disc of HV and LV windings; Cs and Cs' are respectively the series capacitances per disc of the HV and LV winding; Ls and

Ls' are the selfs and mutuals lumped inductances per disc of HV and LV windings; Cw is the Capacitance between HV and LV windings. Theses model parameters can be calculated from FRA [15] or from the transformer's geometrical dimensions [16]. We have neglected the distributed shunt conductance in our model like in [17] and [18]. This approach does not allow us to study the case of leakage fault inside a transformer [14] which is not a problem, since we limit ourselves in this work to: Turn to Turn short circuit; Axial Displacement and Disc Space Variation.

**Table 1:** Comparison Between V-I Method and Others Method Mentioned

| Methods | Allow online diagnosis | Ease of interpretation of results | Identify various internal winding faults |
|---|---|---|---|
| Frequency response analysis [2], [3], [4], [5] | ✓ | | ✓ |
| Analysis of sequences negative current [6] | ✓ | ✓ | |
| Temperature measurement [1], [10] | ✓ | ✓ | |
| Flux based method [9], [12] | ✓ | ✓ | |
| Voltage–current locus diagram V-I [14], [8], [11] | ✓ | ✓ | ✓ |

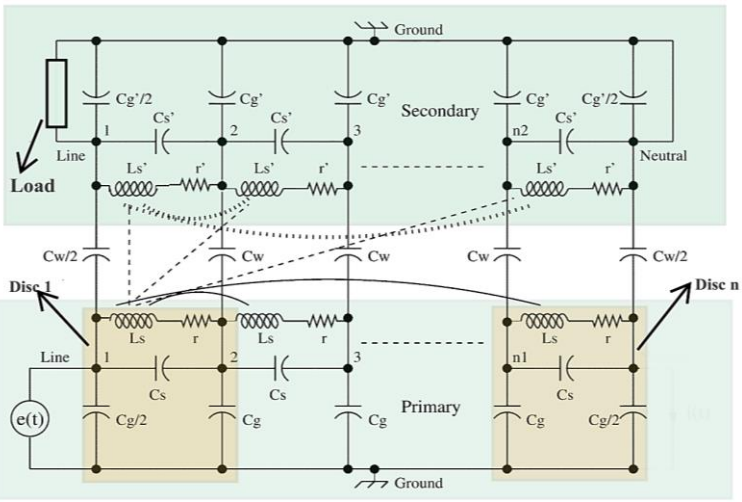


**Fig. 1:** Equivalent Circuit of A Two Winding Transformer Deduce from [17].

Magnetic coupling between the inductances of primary winding
Magnetic coupling between the inductances of primary and secondary winding
Magnetic coupling between the inductances of secondary winding

## 3. Methods

The voltage-current diagram method as presented in [14], [9] relies on constructing a locus diagram (x–y) relating the transformer input current of a particular phase on the x-axis and the difference between the input and output voltages of the same particular phase on the y-axis. In this paper we extend the method to two windings. The current in one primary winding of the transformer is considered as the x-axis, and the voltage difference between primary and secondary is considered as the y-axis. the load and the power factor have little effect on the proposed ΔV-I locus [19], [14].

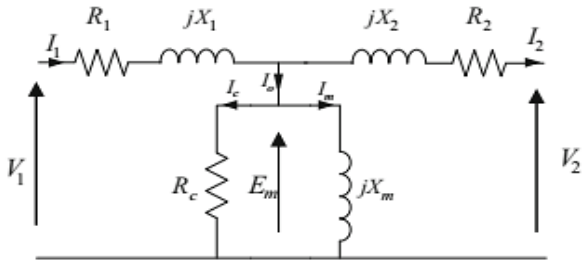


**Fig. 2:** Per-Unit Equivalent Circuit of Transformer.

Considering $\Delta v(t)$ the instantaneous values of the voltage difference between primary $V_1(t)$ and secondary $V_2(t)$ and $i(t)$ the instantaneous input current in one primary phase.
For x-axis:

$$x = i(t) = I_m \cos(\omega t + \varphi) \quad (1)$$

For y-axis:

$$y = V_1(t) - V_2(t) = \Delta v(t) = \Delta V_m \cos(\omega t + \delta) \quad (2)$$

Where $\delta$ and $\varphi$ are the phase angles of $\Delta v(t)$ and $i(t)$, respectively and ω is the angular frequency in rad/s.
We can eliminate from (1) and (2)

$$\omega t = arcos\left(\frac{y}{\Delta V_m}\right) - \delta = arcos\left(\frac{x}{I_m}\right) - \varphi$$

$$\Rightarrow arcos\left(\frac{y}{\Delta V_m}\right) = arcos\left(\frac{x}{I_m}\right) + (\delta - \varphi)$$

$$\Rightarrow \left(\frac{y}{\Delta V_m}\right) = cos\left(arcos\left(\frac{x}{I_m}\right) + (\delta - \varphi)\right)$$

$$\left(\frac{y}{\Delta V_m}\right) = cos\left(arcos\left(\frac{x}{I_m}\right)\right)cos(\delta - \varphi) - sin\left(arcos\left(\frac{x}{I_m}\right)\right)sin(\delta - \varphi) = \left(\frac{x}{I_m}\right)cos(\delta - \varphi) - \sqrt{1 - \left(\frac{x}{I_m}\right)^2}\, sin(\delta - \varphi)$$

$$\Rightarrow \sqrt{1 - \left(\frac{x}{I_m}\right)^2}\, sin(\delta - \varphi) = \left(\frac{x}{I_m}\right)cos(\delta - \varphi) - \left(\frac{y}{\Delta V_m}\right)$$

$$\Rightarrow \left(1 - \left(\frac{x}{I_m}\right)^2\right)sin^2(\delta - \varphi) = \left(\frac{x}{I_m}\right)^2 cos^2(\delta - \varphi) - 2\left(\frac{x}{I_m}\right)cos(\delta - \varphi)\left(\frac{y}{\Delta V_m}\right) + \left(\frac{y}{\Delta V_m}\right)^2$$

$$\Rightarrow sin^2(\delta - \varphi) = \left(\frac{x}{I_m}\right)^2 sin^2(\delta - \varphi) + \left(\frac{x}{I_m}\right)^2 cos^2(\delta - \varphi) - 2\left(\frac{x}{I_m}\right)\left(\frac{y}{\Delta V_m}\right)cos(\delta - \varphi) + \left(\frac{y}{\Delta V_m}\right)^2$$

$$\Rightarrow sin^2(\delta - \varphi) = \left(\frac{x}{I_m}\right)^2 sin^2(\delta - \varphi) + \left(\frac{x}{I_m}\right)^2 cos^2(\delta - \varphi) - 2\left(\frac{x}{I_m}\right)\left(\frac{y}{\Delta V_m}\right)cos(\delta - \varphi) + \left(\frac{y}{\Delta V_m}\right)^2$$

$$\Rightarrow \left(\frac{x}{I_m}\right)^2 - \frac{2xycos(\delta - \varphi)}{I_m \Delta V_m} + \left(\frac{y}{\Delta V_m}\right)^2 = sin^2(\delta - \varphi) \quad (3)$$

$$Ax^2 + Bxy + Cy^2 = F \quad (4)$$

The relationship between x and y in (3) describes the general equation of a conic in (4).
With:

$$A = \frac{1}{{I_m}^2};\ B = \frac{2cos(\delta - \varphi)}{I_m \Delta V_m};\ C = \frac{1}{{\Delta V_m}^2};\ F = sin^2(\delta - \varphi)$$

- If $B^2 - 4AC > 0$ is related to a hyperbola;
- If $B^2 - 4AC < 0$is related to an ellipse;
- If $B^2 - 4AC = 0$ is related to a parabola.

Determine the sign of $B^2 - 4AC$

$$B^2 - 4AC = \frac{4}{{I_m}^2 {\Delta V_m}^2}(cos^2(\delta - \varphi) - 1)$$

$$B^2 - 4AC = -\frac{4}{{I_m}^2 {\Delta V_m}^2}(sin^2(\delta - \varphi)) \quad (5)$$

Equation (5) is always a negative term then the diagram is an ellipse.

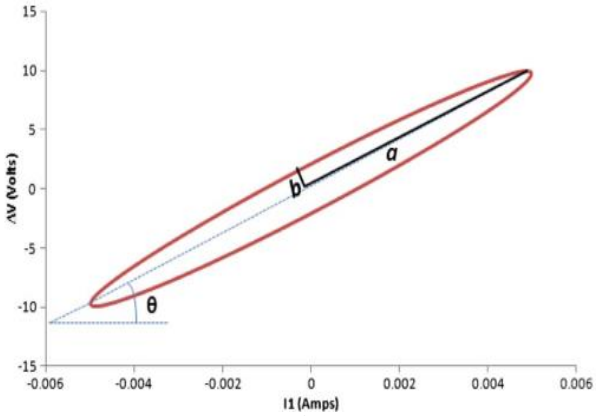


**Fig. 3:** The Form of the Diagram [14].

The parameters of the diagram (the major axis, the minor axis and the rotation angle) are giving in [8]. Their equations are written below

- Rotation angle

$$\theta = \frac{1}{2} artg\left(\frac{B}{A-C}\right) \quad (6)$$

- Semi-major axis

$$a = \sqrt{\frac{-2D}{\left[A+C+D\sqrt{B^2+\left(A-\frac{C}{D}\right)^2}\right]}} \quad (7)$$

- Semi-minor axis

$$b = \sqrt{\frac{-2D}{\left[A+C-D\sqrt{B^2+\left(A-\frac{C}{D}\right)^2}\right]}} \quad (8)$$

- Perimeter (Ramanuja)

$$P \approx \pi\left(3(a+b) - \sqrt{(3a+b)(a+3b)}\right) \quad (9)$$

- Area

$$A = \pi ab \quad (10)$$

The constructed diagram corresponding to the healthy transformer will be compared to the faulty transformer diagram. Three types of internal faults are simulated on the primary winding: Turn to Turn short circuit; Axial Displacement and Disc Space Variation.
We defined the following indicators:

- $R_R$ as the ratio of major axis on the minor axis of the diagram

$$R_R = \frac{a}{b} \quad (11)$$

- $R_\theta$ as the ratio of the faulty diagram angle $\theta_f$ on the healthy diagram angle $\theta$

$$R_\theta = \frac{\theta_f}{\theta} \quad (12)$$

- $R_P$ as the ratio of the faulty diagram perimeter $P_f$ on the healthy diagram perimeter P.

$$R_P = \frac{P_f}{P} \quad (13)$$

- $R_A$ as the ratio of the faulty diagram area $A_f$ on the healthy diagram area A

$$R_A = \frac{A_f}{A} \quad (14)$$

## 4. Simulation results

The power transformer is connected in Δ-Y. 120 HV winding discs and 120 LV winding discs of the model shown in figure 5 are simulated using Matlab/SIMULINK software. As the primary windings are connected in Δ, each extremity of a winding is supplied by 22kV-50Hz, but with a phase difference of 120° as shown in figure 4. The secondary windings are connected in Y with the neutral grounded as shown in figure 4. Two resistors (R) are added between each AC source and the transformer figure 5. These resistors correspond to the line resistance. The value of the RLC parameters of the transformer is given in [18].

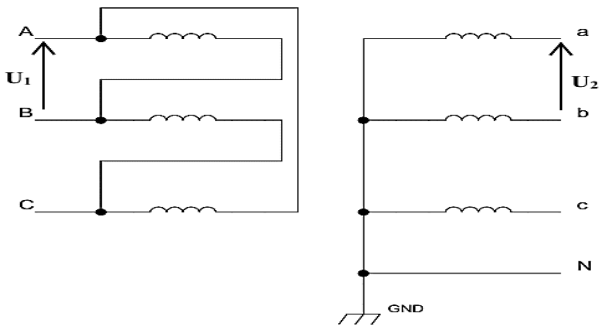


**Fig. 4:** Winding Connection.

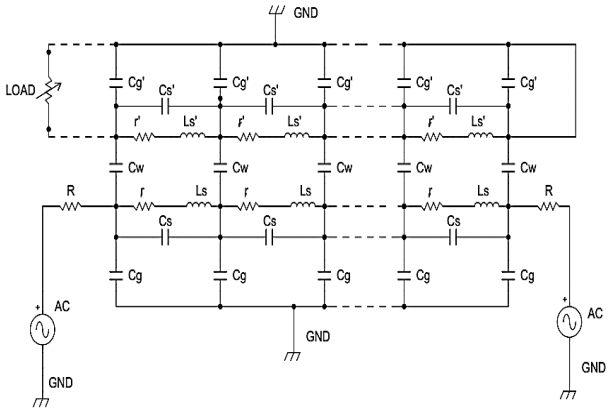


**Fig. 5:** Simulation Model.

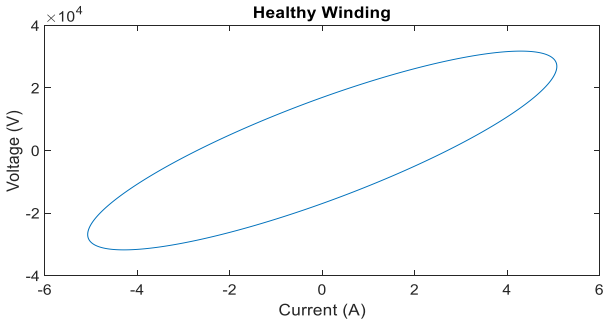


**Fig. 6:** V-I Diagram of the Healthy Winding.

Figure 6 Represent the voltage-current diagram corresponding to the healthy winding. The indicators values are $R_R = 7486.61$; $R_\theta = 1$; $R_P = 1$; $R_A = 1$.

### 4.1. Turn to turn short circuit

About 70 percent of transformers failures are caused by internal winding short-circuit faults [20]. In the model studied, 120 discs were progressively short circuited to find their effect on the diagram.
Figure 7 present the locus for 65, 85, 100 and 120 faulty discs compared to the healthy locus It can be observed from figures 8, 10 and 11 that as the number of faulty disks increase, $R_A$, $R_P$, $R_\theta$ are constant at the value of one until 35 discs are defective, then they start to decrease linearly until 120 discs are defective. $R_R$ evolves in the opposite way as show in figure 9.

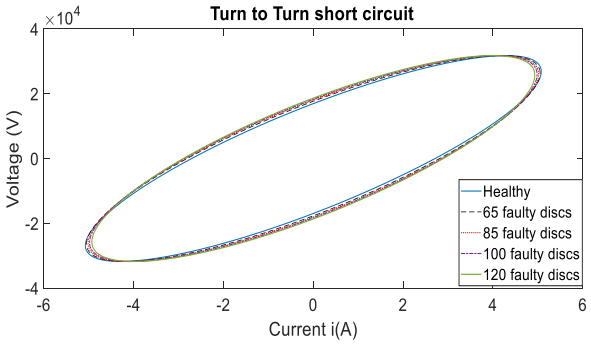


**Fig. 7:** Effect of the Turn-to-Turn Short Circuit Fault on the Locus.

- Ratio of faulty area on healthy area $R_A$

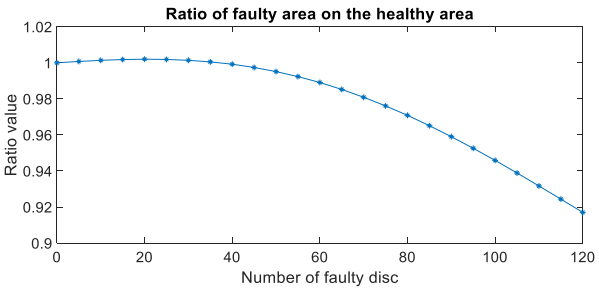


**Fig. 8:** Evolution of the Faulty Area on Healthy Area Ratio.

Using Matlab's curve fitting tool, we can give the expression of this curve by the Fourier method using the Levenberg-Marquardt algorithm.

$$f(x) = a_0 + a_1 \cos(x\omega) + b_1 \sin(x\omega) + a_2 \cos(2x\omega) + b_2 \sin(2x\omega)$$

Coefficients (with 95% confidence bounds):

$a_0 = 1{,}459\ (-1{,}222;\ 4{,}14)$

$a_1 = -0{,}6254\ \ (-4{,}215;\ 2{,}964)$

$b_1 = -0{,}418\ \ (-1{,}854;\ 1{,}018)$

$a_2 = 0{,}1659\ \ (-0{,}7427;\ 1{,}075)$

$b_2 = 0{,}2195\ \ (-0{,}5081;\ 0{,}9471)$

$\omega = 0{,}007598\ \ (3{,}323e^{-05};\ 0{,}01516)$

The RMSE = 2,453e$^{-05}$

- Ratio of major axis on minor axis $\boldsymbol{R_R}$

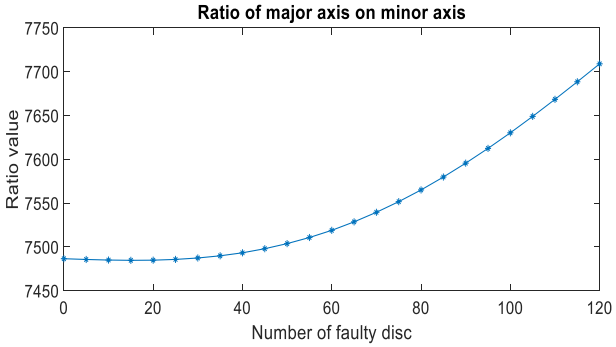


**Fig. 9:** Evolution of the Major Axis on Minor Axis Ratio.

The expression of this curve by the Fourier method using the Levenberg-Marquardt algorithm (Matlab).

$$f(x) = a_0 + a_1 \cos(x\omega) + b_1 \sin(x\omega) + a_2 \cos(2x\omega) + b_2 \sin(2x\omega)$$

Coefficients (with 95% confidence bounds):

$a_0 = 7049\ \ (6278;\ 7819)$

$a_1 = 587{,}4\ (-432{,}2;\ 1607)$

$b_1 = 729{,}8\ (155{,}7\ ;\ 1304)$

$a_2 = -149{,}3\ \ (-398{,}5;\ 99.82)$

$b_2 = -375{,}4\ \ (-663{,}9;\ -86{,}89)$

$\omega = 0{,}008475\ \ (0{,}00664;\ 0{,}01031)$

The RMSE: 0,03793

- Ratio of faulty angle on healthy angle $\boldsymbol{R_\theta}$

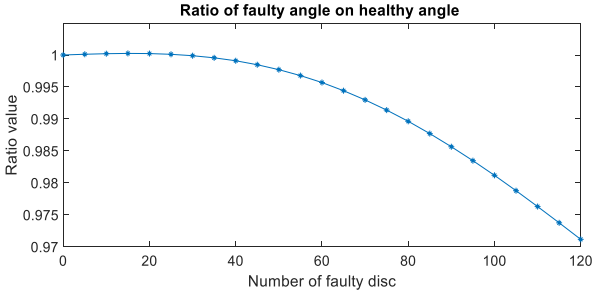


**Fig. 10:** Evolution of the Faulty Angle on the Healthy Angle Ratio.

The expression of this curve by the Fourier method using the Levenberg-Marquardt algorithm (Matlab).

$$f(x) = a_0 + a_1\cos(x\omega) + b_1\sin(x\omega) + a_2\cos(2x\omega) + b_2\sin(2x\omega)$$

Coefficients (with 95% confidence bounds):

$a_0 = 1{,}12\ \ (0{,}8365;\ 1{,}404)$

$a_1 = -0{,}1601\ \ (-0{,}5364;\ 0{,}2161)$

$b_1 = -0{,}1325\ \ (-0{,}3058;\ 0{,}04077)$

$a_2 = 0{,}04003\ \ (-0{,}05266;\ 0{,}1327)$

$b_2 = 0{,}06775\ \ (-0{,}01931;\ 0{,}1548)$

$\omega = 0{,}007814\ \ (0{,}004864;\ 0{,}01076)$

The RMSE: 5,602e$^{-06}$

- Ratio of faulty perimeter on the healthy perimeter $\boldsymbol{R_P}$

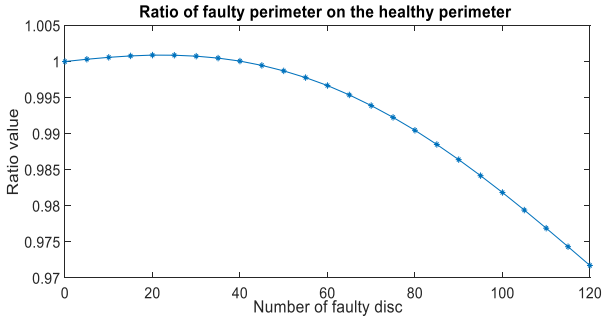


**Fig. 11:** Evolution of the Faulty Perimeter on the Healthy Perimeter Ratio.

The expression of this curve by the Fourier method using the Levenberg-Marquardt algorithm (Matlab).

$$f(x) = a_0 + a_1\cos(x\omega) + b_1\sin(x\omega) + a_2\cos(2x\omega) + b_2\sin(2x\omega)$$

Coefficients (with 95% confidence bounds):

$a_0 = 1{,}213\ \ (-0{,}01103;\ 2{,}437)$

$a_1 = -0{,}291\ \ (-1{,}934;\ 1{,}352)$

$b_1 = -0{,}1728\ \ (-0{,}7775;\ 0{,}432)$

$a_2 = 0{,}07806\ \ (-0{,}3408;\ 0{,}497)$

$b_2 = 0{,}09115\ \ (-0{,}2159;\ 0{,}3982)$

$\omega = 0{,}007048\ (-0{,}0001682\ ;\ 0{,}01426)$

RMSE: 7,179e$^{-06}$

- Axial displacement

This fault occurs due to the magnetic imbalance between the low- and high-voltage windings due to short-circuit currents [14]. This fault can be simulated by modifying the mutual inductances and self-inductances of disc [9]. In the model studied, axial displacement is modelled by reducing the inductance by 10%. Axial displacement was progressively simulated on 120 discs to find its effect on the diagram. Figure 12 present the locus for 50, 80, 100 and 120 faulty disks compared to the healthy locus It can be observed from figures 13, 15 and 16 that as the number of faulty disks increase, $R_A$, $R_P$, $R_\theta$ are increasing linearly in the same direction. $R_R$ evolves in the opposite way as shown in figure 14.

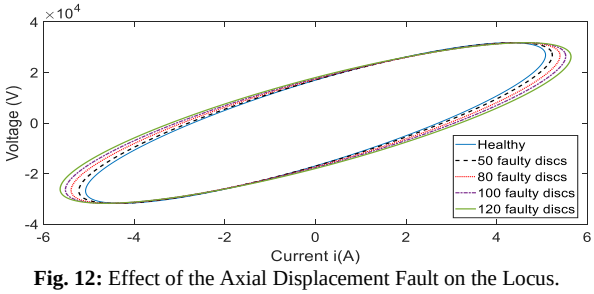


**Fig. 12:** Effect of the Axial Displacement Fault on the Locus.

- Ratio of faulty area on healthy area $R_A$

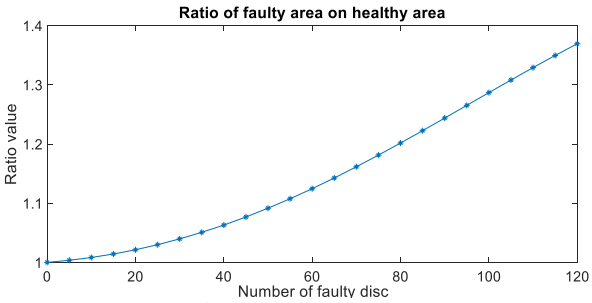


**Fig. 13:** Evolution of the Faulty Area on Healthy Area Ratio.

The expression of this curve by the Fourier method using the Levenberg-Marquardt algorithm (Matlab) number of terms 1.

$$f(x) = a_0 + a_1 \cos(x\omega) + b_1 \sin(x\omega)$$

Coefficients (with 95% confidence bounds):

$a_0 = 1{,}291 \ \ (1{,}281;\ 1{,}301)$

$a_1 = -0{,}2894 \ \ (-0{,}2998;\ -0{,}279)$

$b_1 = 0{,}023 \ \ (0{,}0182;\ 0{,}0278)$

$\omega = 0{,}01475 \ \ (0{,}01429;\ 0{,}01521)$

The RMSE: 0,000695

- Ratio of major axis on minor axis $R_R$

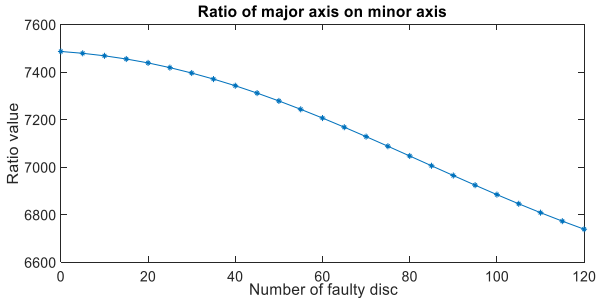


**Fig. 14:** Evolution of the Major Axis on Minor Axis Ratio.

The expression of this curve by the Fourier method using the Levenberg-Marquardt algorithm (Matlab) number of term 1.

$$f(x) = a_0 + a_1 \cos(x\omega) + b_1 \sin(x\omega)$$

Coefficients (with 95% confidence bounds):

$a_0 = 7018 \ \ (7015;\ 7021)$

$a_1 = 467{,}2 \ \ (463{,}9;\ 470{,}6)$

$b_1 = -52{,}42 \ \ (-55{,}54;\ -49{,}29)$

$\omega = 0{,}01746 \ \ (0{,}01732;\ 0{,}0176)$

RMSE: 0,5385

- Ratio of faulty angle on healthy angle $R_\theta$

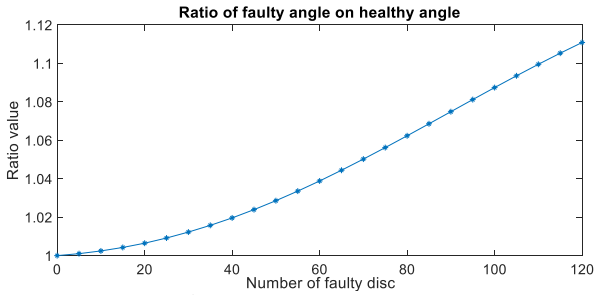


**Fig. 15:** Evolution of the Faulty Angle on the Healthy Angle Ratio.

The expression of this curve by the Fourier method using the Levenberg-Marquardt algorithm (Matlab) number of term 1.

$$f(x) = a_0 + a_1 \cos(x\omega) + b_1 \sin(x\omega)$$

Coefficients (with 95% confidence bounds):

$a_0 = 1{,}077 \ \ (1{,}076;\ 1{,}079)$

$a_1 = -0{,}07692 \ \ (-0{,}07838;\ -0{,}07546)$

$b_1 = 0{,}00614 \ \ (0{,}00521;\ 0{,}00707)$

$\omega = 0{,}01621 \ \ (0{,}01591;\ 0{,}01651)$

The RMSE: 0,0001525

- Ratio of faulty perimeter on the healthy perimeter $\boldsymbol{R_P}$

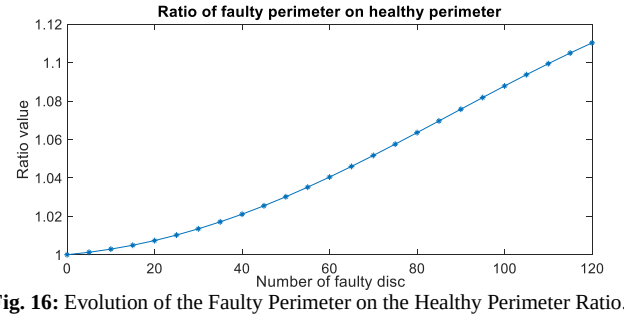


**Fig. 16:** Evolution of the Faulty Perimeter on the Healthy Perimeter Ratio.

The expression of this curve by the Fourier method using the Levenberg-Marquardt algorithm (Matlab) number of terms 1.

$$f(x) = a_0 + a_1 \cos(x\omega) + b_1 \sin(x\omega)$$

Coefficients (with 95% confidence bounds):

$a_0 = 1{,}075 \ \ (1{,}074;\ 1{,}076)$

$a_1 = -0{,}07435 \ \ (-0{,}07548;\ -0{,}07323)$

$b_1 = 0{,}009668 \ \ (0{,}008821;\ 0{,}01052)$

$\omega = 0{,}01616 \ \ (0{,}01591;\ 0{,}01642)$

The RMSE: 0, 0001285

### 4.2. Disc space variation

Disc space variation is one of the most frequently mechanical faults occurring in power transformers [14]. This fault can be simulated by modifying the series capacitor [14]. In the model studied, Disc space variation is modelled by increasing the series capacitor by 70%. Disc space variation was progressively simulated on 120 to find its effect on the diagram.
Figure 17 present the locus for 50, 80, 100 and 120 faulty discs compared to the healthy locus. It can be observed from figures 18, 19, 20 and 21 that as the number of faulty disks increase, $R_A$, $R_P$, $R_\theta$, $R_R$ are constant. this may mean that the method does not allow the assessment of this fault or that further study would help to understand this phenomenon.

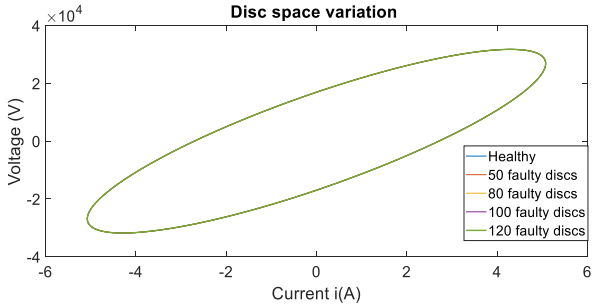


**Fig. 17:** Effect of Disc Space Variation Fault on the Locus.

- Ratio of faulty area on healthy area $R_A$

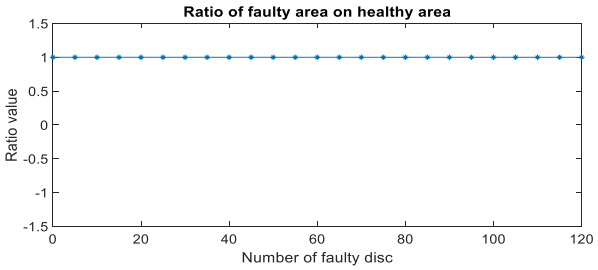


**Fig. 18:** Evolution of the Faulty Area on Healthy.

- Ratio of major axis on minor axis $R_R$

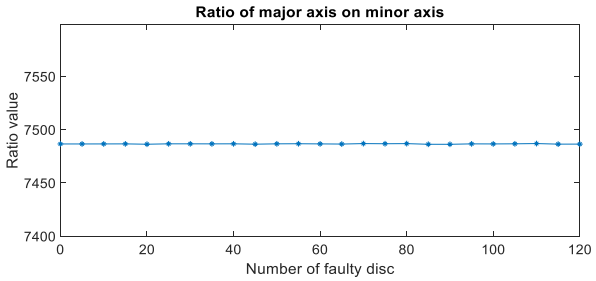


**Fig. 19:** Evolution of the Ratio of Major Axis on Minor Axis.

- Ratio of faulty angle on healthy angle $R_\theta$

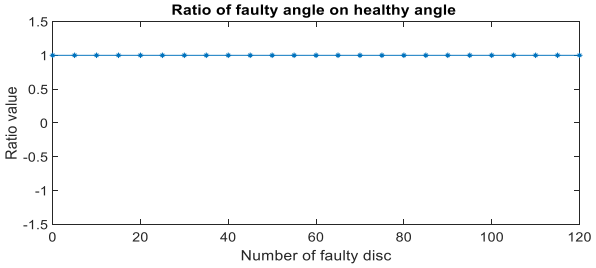


**Fig. 20:** Evolution of the Faulty Angle on The Healthy Angle Ratio.

- Ratio of faulty perimeter on the healthy perimeter $R_P$

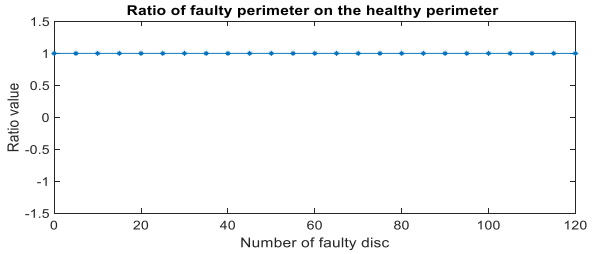


**Fig. 21:** Evolution of the Faulty Perimeter on the Healthy Perimeter Ration.

## 5. Conclusion

This paper presents the diagnosis of a 15 MVA 22/0.415 kV distribution power transformer by the voltage-current locus diagram method. The method Consist of establishing a locus diagram (x–y) where current in one primary winding of the transformer is considered as the x-axis, and the voltage difference between primary and secondary is considered as the y-axis. Three types of faults have been simulated using Matlab/Simulink software: short-circuit faults, Axial displacement and disc space variation. for each fault and at different number of faulty discs we determined: the major axis, minor axis, perimeter, area and inclination angle of the diagram. These parameters allow us to defined four indicators $R_A$, $R_P$, $R_\theta$, and $R_R$. The analysis of these indicators made possible the identification of each fault and its mathematical model. This technique is very easy to implement. It requires only the metering devices attached to the power transformer and can be done online. The application of this method to other electrical equipment may be the subject of future research.

## References


[1] Aslam, M., Haq, I.U., Rehan, M.S., Ali, F., Basit, A., Khan, M.I., Arbab, M.N., 2021. Health Analysis of Transformer Winding Insulation Through Thermal Monitoring and Fast Fourier Transform (FFT) Power Spectrum. IEEE Access 9, 114207–114217. https://doi.org/10.1109/ACCESS.2021.3104033.

[2] 16- Wang, M., 2003. Winding movement and condition monitoring of power transformers in service. University of British Columbia.

[3] Behjat, V., Vahedi, A., Setayeshmehr, A., Borsi, H., Gockenbach, E., 2011. Diagnosing Shorted Turns on the Windings of Power Transformers Based Upon Online FRA Using Capacitive and Inductive Couplings. IEEE Transactions on Power Delivery - IEEE TRANS POWER DELIVERY 26, 2123–2133. https://doi.org/10.1109/TPWRD.2011.2151285.

[4] Liu, Y., Ji, S., Yang, F., Cui, Y., Zhu, L., Rao, Z., Ke, C., Yang, X., 2015. A study of the sweep frequency impedance method and its application in the detection of internal winding short circuit faults in power transformers. IEEE Trans. Dielect. Electr. Insul. 22, 2046–2056. https://doi.org/10.1109/TDEI.2015.004977.

[5] Tahir, M., Tenbohlen, S., 2021. Transformer Winding Condition Assessment Using Feedforward Artificial Neural Network and Frequency Response Measurements. Energies 14, 3227. https://doi.org/10.3390/en14113227.

[6] Babiy, M., Gokaraju, R., Garcia, J.C., 2011. Turn-to-turn fault detection in transformers using negative sequence currents, in 2011 IEEE Electrical Power and Energy Conference. Presented at the Energy Conference (EPEC), IEEE, Winnipeg, MB, Canada, pp. 158–163. https://doi.org/10.1109/EPEC.2011.6070187.

[7] Abu-Siada, A., Islam, S., 2012. A Novel Online Technique to Detect Power Transformer Winding Faults. IEEE Trans. Power Delivery 27, 849–857. https://doi.org/10.1109/TPWRD.2011.2180932.

[8] Zhao, X., Yao, C., Zhou, Z., Li, C., Wang, X., Zhu, T., Abu-Siada, A., 2020. Experimental Evaluation of Transformer Internal Fault Detection Based on V–I Characteristics. IEEE Transactions on Industrial Electronics 67, 4108–4119. https://doi.org/10.1109/TIE.2019.2917368.

[9] Chong, J., Abu-Siada, A., 2011. A novel algorithm to detect internal transformer faults, in: 2011 IEEE Power and Energy Society General Meeting. Presented at the 2011 IEEE Power & Energy Society General Meeting, IEEE, San Diego, CA, pp. 1–5. https://doi.org/10.1109/PES.2011.6039472.

[10] Hurezeanu, I., Nicola, C., Sacerdotianu, D., Nicola, M., Aciu, A.-M., Nitu, M.C., 2016. Temperature control and monitoring system for power transformer windings using fiber optic sensors. https://doi.org/10.1109/ISFEE.2016.7803151.

[11] Haghjoo, F., Mostafaei, M., 2016. Flux-based method to diagnose and identify the location of turn-to-turn faults in transformers. IET Generation, Transmission & Distribution 10, 1083–1091. https://doi.org/10.1049/iet-gtd.2015.1180.

[12] Mostafaei, M., Haghjoo, F., 2016. Flux-based turn-to-turn fault protection for power transformers. IET Generation, Transmission & Distribution 10, 1154–1163. https://doi.org/10.1049/iet-gtd.2015.0738.

[13] Small, B.J., Abu-Siada, A., 2011. A new method for analysing transformer condition using frequency response analysis, in: 2011 IEEE Power and Energy Society General Meeting. Presented at the 2011 IEEE Power & Energy Society General Meeting, IEEE, San Diego, CA, pp. 1–5. https://doi.org/10.1109/PES.2011.6039470.

[14] Abu-Siada, A., Islam, S., 2012. A Novel Online Technique to Detect Power Transformer Winding Faults. IEEE Trans. Power Delivery 27, 849–857. https://doi.org/10.1109/TPWRD.2011.2180932.

[15] Dick, E.P., Erven, C.C., 1978. Transformer Diagnostic Testing by Frequuency Response Analysis. IEEE Trans. on Power Apparatus and Syst. PAS-97, 2144–2153. https://doi.org/10.1109/TPAS.1978.354718.

[16] Zhao, C., Ruan, J., Du, Z., Liu, S., Yu, Y., Zhang, Y., 2008. Calculation of parameters in transformer winding based on the model of multi-conductor transmission line, in 2008 International Conference on Electrical Machines and Systems. Presented at the 2008 International Conference on Electrical Machines and Systems, pp. 463–467.

[17] Ragavan, K., Satish, L., 2005. An efficient method to compute transfer function of a transformer from its equivalent circuit. IEEE Transactions on Power Delivery 20, 780–788. https://doi.org/10.1109/TPWRD.2004.834345.

[18] Ibrahim, K.H., Korany, N.R., Saleh, S.M., 2022. Effects of power transformer high-frequency equivalent circuit parameters non-uniformity on fault diagnosis using SFRA test. Ain Shams Engineering Journal 13, 101674. https://doi.org/10.1016/j.asej.2021.101674.

[19] Abbasi, A.R., 2022. Fault detection and diagnosis in power transformers: a comprehensive review and classification of publications and methods. Electric Power Systems Research 209, 107990. https://doi.org/10.1016/j.epsr.2022.107990.

[20] Yazdani Asrami, M., Samadaei, E., Darvishi, S., Taghipour, M., 2010. Modeling and simulation of transformer winding fault using MATLAB/SIMULINK. International Review on Modelling and Simulations 3, 1103–1109.